Hindawi Publishing Corporation
International Journal of Photoenergy
Volume 2014, Article ID 539414, 13 pages
http://dx.doi.org/10.1155/2014/539414

Research Article

Optimal Capacity Allocation of Large-Scale Wind-PV-Battery Units

Kehe Wu,[1,2] Huan Zhou,[2] and Jizhen Liu[1,2]

[1] *State Key Laboratory of Alternate Electrical Power System with Renewable Energy Sources, North China Electric Power University, Beijing 102206, China*
[2] *School of Control and Computer Engineering, North China Electric Power University, P.O. Box 570, Beijing 102206, China*

Correspondence should be addressed to Huan Zhou; shenarder@163.com

Received 10 December 2013; Revised 5 February 2014; Accepted 19 February 2014; Published 17 April 2014

Academic Editor: Mahmoud M. El-Nahass

An optimal capacity allocation of large-scale wind-photovoltaic- (PV-) battery units was proposed. First, an output power model was established according to meteorological conditions. Then, a wind-PV-battery unit was connected to the power grid as a power-generation unit with a rated capacity under a fixed coordinated operation strategy. Second, the utilization rate of renewable energy sources and maximum wind-PV complementation was considered and the objective function of full life cycle-net present cost (NPC) was calculated through hybrid iteration/adaptive hybrid genetic algorithm (HIAGA). The optimal capacity ratio among wind generator, PV array, and battery device also was calculated simultaneously. A simulation was conducted based on the wind-PV-battery unit in Zhangbei, China. Results showed that a wind-PV-battery unit could effectively minimize the NPC of power-generation units under a stable grid-connected operation. Finally, the sensitivity analysis of the wind-PV-battery unit demonstrated that the optimization result was closely related to potential wind-solar resources and government support. Regions with rich wind resources and a reasonable government energy policy could improve the economic efficiency of their power-generation units.

1. Introduction

Wind and solar energy are forms of green energy with tremendous application prospects. At present, some countries have started research on the key technical problems of wind-photovoltaic- (PV-) battery units [1–4]. In 2011, China established a demonstration wind-PV-battery unit in Zhangbei; this project aims to explore the stability and economic efficiency of large-scale power grids with renewable energy sources [5].

Numerous studies on optimizing the capacity of wind-PV-battery units have been reported. These studies can be mainly divided into single and multiple objective optimizations. The former primarily considers power distribution reliability as a constraint and targets minimum investment cost. For example, aiming to reduce net present cost of distribution systems, Mohammadi et al. suggested using particle swarm optimization to optimize the capacities of distributed generators in a microgrid under different market policies [6]. To minimize the annual cost of a system, Yang et al. considered the expected power shortage rate as a constraint and established an independent capacity optimization model for wind-PV-battery units. He applied the model in a communication relay station in the southeastern coastal areas in China and thus confirmed the feasibility of his model [7–9]. Diaf et al. established an independent economic optimization model for wind-PV-battery units to minimize the levelized cost of energy (LCE) and to analyze the sensitivity factors of wind-PV-battery units [10].

Multiple objective optimizations mainly aim to improve investment cost and power distribution reliability. Moreover, they consider environmental protection, such as reducing exhaust emissions. For example, Kazem and Khatib calculated the optimal capacity ratio of a wind-PV-diesel-battery power-generation system through a numerical algorithm to minimize cost and maximize power distribution reliability. They verified the economic efficiency and feasibility of their optimal capacity ratio through the power supply system in several communities in Oman [11]. Aiming at a minimum life cycle cost with no load shedding, Li et al. used

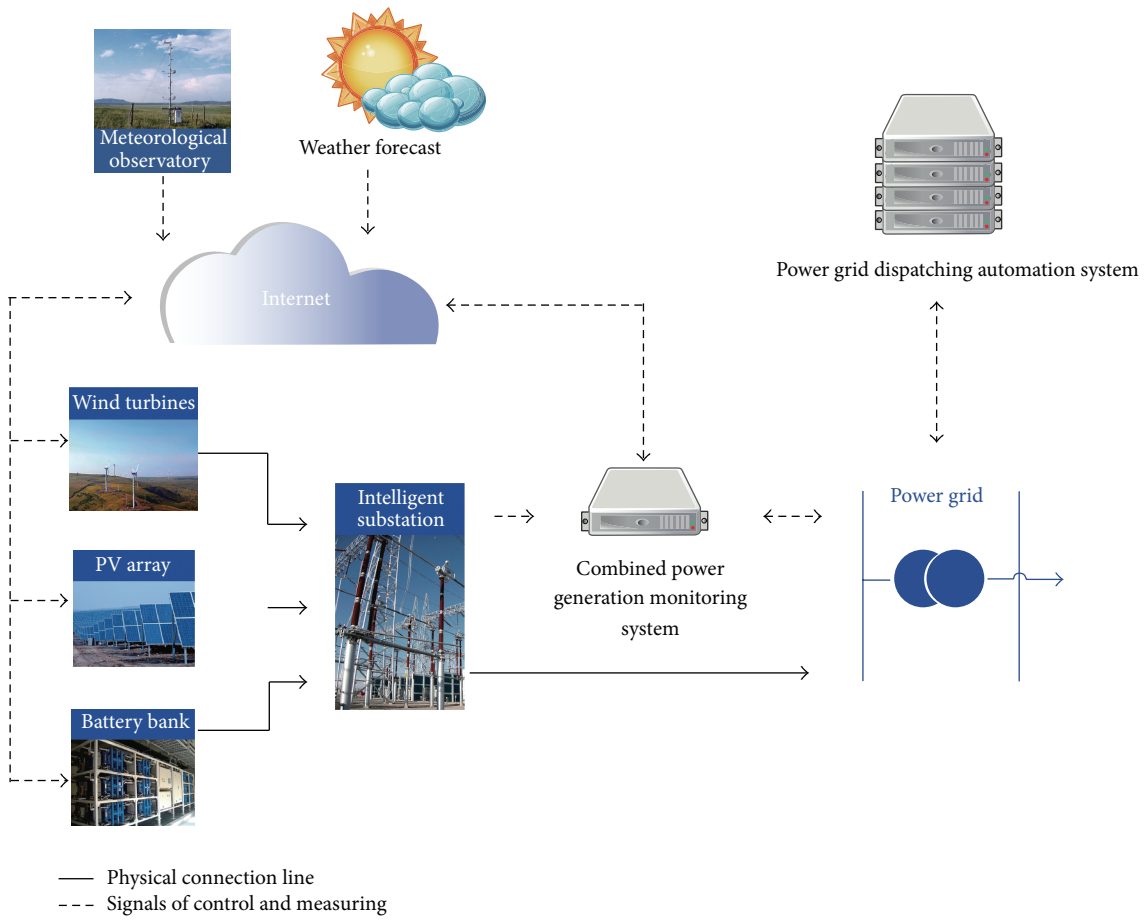

Figure 1: Basic structure of wind-PV-battery units.

a simple sizing algorithm to calculate the capacity allocation of an independent wind-PV-battery unit and determined that the state of charge (SOC) of a battery should be periodically invariant. They confirmed the reliability and economic efficiency of the algorithm through a case study in Zhoushan Island, China [12]. To minimize the LCE and CO_2 emissions within equivalent life cycles, Dufo-López et al. adopted a multiobjective evolutionary algorithm to calculate the optimal capacity ratio of a wind-PV-diesel-battery power-generation system [13, 14]. To minimize system cost and loss of power supply probability, Khatiba et al. calculated the optimal capacity ratio of a wind-PV-battery unit in a microgrid environment by using a genetic algorithm (GA). Moreover, they further optimized the hub height of a wind turbine and the optimal tilt angle of the PV array [15].

Previous studies on the capacity allocation of wind-PV-battery units have mainly focused on allocating appropriate wind-PV capacity ratios to achieve a wind-PV output power that is as close as possible to the load curve as well as to reduce charge-discharge times and the discharge depth of the battery. The capacity allocation and characteristics of the overall output power are closely related to the load variation trend, thus significantly restricting its application in large-scale wind-PV-battery units. During the grid-connected operation of a large-scale wind-PV-battery unit, the power grid has to consider the unit as a power plant with a particular rated capacity to perform corresponding dispatcher tasks. In the present study, an optimal capacity allocation of wind-PV-battery units based on a rate capacity was proposed to minimize the net present cost (NPC). The optimal capacity of each wind-PV-battery unit under a rated capacity was calculated by using a HIAGA.

2. Operating Model of the Wind-PV-Battery Units

2.1. System Structure. The wind-PV-battery units mainly consist of a combined power-generation monitoring system, a wind generator, a PV array, and a battery-energy storage device. The basic structure is shown in Figure 1.

The wind generator and the PV array are primarily responsible for generating power from renewable energy sources such as wind and solar energy, whereas the battery is responsible for maintaining a stable overall power output of the wind-PV-battery units through peak clipping and valley filling. The combined power-generation monitoring system provides a reasonable arrangement of the power-generation devices according to dispatching commands and weather forecasts (e.g., wind speed, illumination intensity,

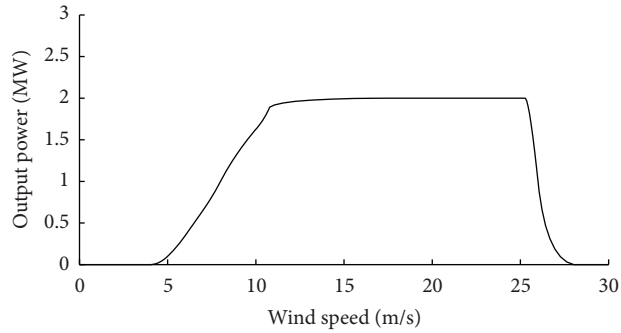

Figure 2: Output power characteristics of the wind generator.

and temperature), thus ensuring the stable grid-connected operation of the wind-PV-battery units.

2.2. Output Power Model of the Wind Generator. The output power model of the wind generator is closely related to site conditions such as surface roughness and tower height. Given that the actual wind speed at the hub is different from that at the monitoring point [16], the measured wind speed has to be converted through

$$v(k) = v_{\text{ref}}\left[\frac{H}{H_{\text{ref}}}\right]^{\alpha}, \tag{1}$$

where v_{ref} and $v(k)$ are the measured wind speed at the monitoring point and the wind speed at the hub at k; H and H_{ref} are the hub height and the monitoring height, respectively; and α (1/7 to 1/4) is the descriptive factor of surface roughness, which is determined by the surface environment of the wind generator.

The actual output power of the wind generator is closely related to wind speed (Figure 2). The output power characteristics of the wind generator can be expressed as

$$P_{\text{wd}}(k) = \begin{cases} 0, & v(k) < v_{\min} \text{ or } v(k) > v_{\max}, \\ P_{\text{rated}}, & v_{\text{rated}} \le v(k) \le v_{\max}, \\ P_{\text{rated}} \dfrac{v(k)^2 - v_{\min}^2}{v_{\text{rated}}^2 - v_{\min}^2}, & v_{\min} \le v(k) < v_{\text{rated}}, \end{cases} \tag{2}$$

where $P_{\text{wd}}(k)$ is the output power of the wind generator at k; P_{rated} is the rated power of the wind generator; and $v_{\min}$, $v_{\max}$, and v_{rated} are the minimum start-up wind speed, cutoff wind speed, and minimum rated wind speed of the wind generator.

2.3. Output Power Model of the PV Module. The output power model of the PV module is determined by solar radiation and environmental temperature as follows [6]:

$$P_{\text{PV}}(t) = A_{\text{PV}} G(t) \eta_{\text{PV}}(t) \eta_{\text{inv}}, \tag{3}$$

where A_{PV} (m^2) is the area of the PV panel exposed to solar radiation, $G(t)$ (W/m^2) is the value of solar radiation, $\eta_{\text{PV}}(t)$ is the energy conversion efficiency of the PV module, and η_{inv} is the conversion efficiency of the inverter. $\eta_{\text{PV}}(t)$ is influenced by environmental temperature:

$$\eta_{\text{PV}}(t) = \eta_{\text{ref}}\left[1 - \beta\left(T_C(t) - T_{C_{\text{ref}}}\right)\right], \tag{4}$$

where η_{ref} is the reference energy conversion efficiency of the PV module under a standard temperature, β is the influence coefficient of the temperature for energy conversion efficiency, $T_C(t)$ is the temperature of the PV module at t, and $T_{C_{\text{ref}}}$ is the reference standard temperature of the PV module. The temperature of the PV module changes under the influence of solar radiation absorption and environmental temperature as follows:

$$T_C(t) - T_{\text{ambient}} = \frac{T_{\text{rated}}}{800} G(t), \tag{5}$$

where T_{ambient} is the ambient temperature and T_{rated} is the rated temperature of the PV module.

2.4. Battery Model. Given that the battery devices of large-scale wind-PV-battery units can be concentrated in an independent plant with a constant indoor temperature, the charge and discharge efficiencies of the battery are not affected by temperature. The output power model of the battery is [17] as follows:

(1) charge

$$\text{Soc}(t) = \text{Soc}(t-1)(1-\sigma) + \frac{P_c(t)\Delta t \eta_c}{E_{\max}}, \tag{6}$$

(2) discharge

$$\text{Soc}(t) = \text{Soc}(t-1)(1-\sigma) - \frac{P_d(t)\Delta t}{E_{\max}\eta_d}, \tag{7}$$

where $\text{Soc}(t)$ is the battery level after t; σ is the self-discharge per hour of the battery; P_c and P_d are the charge and discharge powers of the battery in t, respectively; Δt is the length of t; η_c and η_d are the charge and discharge efficiencies of the battery, respectively; and $E_{\max}$ is the maximum capacity of the battery.

The modeling of the life cycle of a battery will affect the calculation of total system cost. Existing literature has established the life cycle expectancy model of batteries based on battery operations and charge-discharge strategies under a constant temperature [18]. The present study adopts the method of Lopez [11] which estimates cycles to failure of batteries by calculating the number of charge and discharge within an interval of several discharge depths (Figure 3).

The life cycle of a battery can be calculated according to the following equation:

$$\text{Life}_{\text{bat}} = \frac{1}{\sum_{i=1}^{m}\left(N_i/\text{CF}_i\right)}, \tag{8}$$

where m is the total interval, N_i is the number of charge and discharge of the battery within interval i, and CF_i is the cycles to failure within interval i.

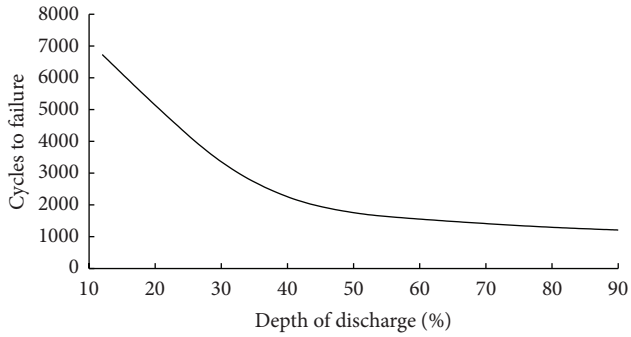

Figure 3: Battery cycle.

The replacement cycle of a battery (Y_{RES}) can be expressed as

$$Y_{\mathrm{RES}} = \min\left\{\mathrm{Life}_{\mathrm{bat}}, \mathrm{Life}_{\mathrm{float}}\right\}, \tag{9}$$

where $\mathrm{Life}_{\mathrm{float}}$ is the float life of a battery that is provided by manufacturers.

3. Optimization Model

3.1. Coordinated Operating Strategy. The wind-PV-battery unit controls the battery device through the principle of maximum utilization of renewable energy sources and constant output power. When the wind-PV output power is smaller than the dispatching demand (P_{ref}), the remaining power is replenished through battery discharge. Battery devices stop active output power until they reach the maximum discharge depth ($\mathrm{Soc}_{\mathrm{min}}$).

Consider

$$P_d(t) = P_{\mathrm{ref}} - \left[P_{\mathrm{wd}}(t) + P_{\mathrm{PV}}(t)\right], \quad \mathrm{Soc}(t) > \mathrm{Soc}_{\mathrm{min}}, \tag{10}$$

where $P_d(t)$ can be deduced from (7).

When the wind-PV output power is higher than P_{ref}, surplus energy is stored in the battery. Battery devices stop charging when they are fully charged ($\mathrm{Soc}_{\mathrm{max}}$).

Consider

$$P_c(t) = \left[P_{\mathrm{wd}}(t) + P_{\mathrm{PV}}(t)\right] - P_{\mathrm{ref}}, \quad \mathrm{Soc}(t) < \mathrm{Soc}_{\mathrm{max}}, \tag{11}$$

where $P_c(t)$ can be deduced from (6).

3.2. Optimization Variables. The numbers of wind generators (N_{wd}), PV modules (N_{PV}), and battery devices (N_{bat}) involved in the wind-PV-battery unit are selected as optimization variables and recorded as

$$X = \left[N_{\mathrm{wd}} \quad N_{\mathrm{PV}} \quad N_{\mathrm{bat}}\right]^T. \tag{12}$$

3.3. Objective Function. The reliable and high-quality electric power supply with renewable energy sources, optimal environmental protection, and maximum economic benefits are the development goals of new-energy power enterprises. The goals of the optimal capacity allocation of large-scale wind-PV-battery power-generation unit designed in this paper include minimum total investment cost, maximum utilization rate of renewable energy sources, minimum environmental cost, maximum power distribution reliability.

From the analysis of these goals, we can conclude that, firstly, wind-PV-battery unit does not include the traditional fossil energy. Therefore, environmental pollution will not be taken into consideration. Secondly, the guarantee of the constant output power is beneficial to the improvement of the grid-connected operation reliability of large-scale new energy. Finally, the maximum utilization rate of renewable energy sources and less installed capacity of battery contribute to the reduction of total investment cost. In the following analysis, the reliability and energy utilization rate are considered as the constraints of the system performance, instead of the optimal goals. In this way, it can not only shrink the scope of algorithmic search solution space, but also enable the system performance of each component to reach a relative balance. The designed wind-PV-battery unit aims to minimize the NPC as follows [19]:

$$C_{\mathrm{NPC}} = \sum_{k=1}^{K} \frac{C_{\mathrm{OUT}}(k) - C_{\mathrm{IN}}(k)}{(1+r)^k}, \tag{13}$$

where K is the service life of the project; r is discount rate; and $C_{\mathrm{OUT}}(k)$ and $C_{\mathrm{IN}}(k)$ are the costs and revenues of the unit at kth year, respectively, which are calculated through the following equations:

$$\begin{aligned} C_{\mathrm{OUT}} &= C_I + C_{OM}(k) + C_R(k), \\ C_{OM}(k) &= \sum_{i=1}^{3} C_O\left(x_i, t_i^O\right) + \sum_{i=1}^{3} C_M\left(x_i, t_i^M\right), \\ C_R(k) &= \sum_{i=1}^{3} C_R\left(x_i, k\right), \\ C_{\mathrm{IN}}(k) &= P_S \int_0^T P_{\mathrm{wpb}}(t)\, dt + C_{\mathrm{salvage}}, \end{aligned} \tag{14}$$

where C_I is the initial cost; C_O and C_M are the operation and maintenance costs of equipment, respectively; t_i^O and t_i^M are the operation time and maintenance time of equipment i, respectively; $C_R(x_i, k)$ is the replacement cost of equipment i at kth year; $P_{\mathrm{wpb}}(t)$ is the accessing power of renewable energy at t; P_S is the corresponding feed-in tariff; and C_{salvage} is the remanent value of equipment.

3.4. Performance Constraints

(1) Power Balance Constraint. The overall accessing power of the wind-PV-battery unit should be consistent with the expected accessing power (P_{ref}) during dispatching at all times; that is,

$$P_{\mathrm{ref}} = P_{\mathrm{wd}}(t) + P_{\mathrm{PV}}(t) + P_{\mathrm{bat}}(t), \tag{15}$$

where $P_{\mathrm{wd}}(t)$, $P_{\mathrm{PV}}(t)$, and $P_{\mathrm{bat}}(t)$ are the output power of the wind generator, the PV module, and the battery devices at t, respectively.

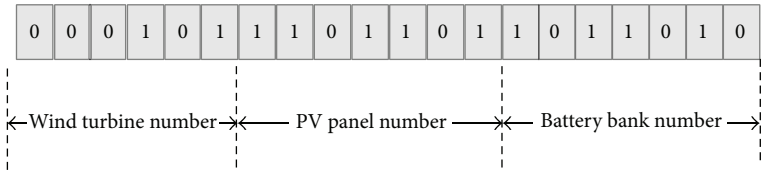

Figure 4: Binary coding of optimization variables.

(2) Loss of Produced Power Probability Constraint. The wind-PV-battery unit should take full advantage of renewable energy sources to reduce waste of energy and to limit loss of produced power probability (R_{LPPP}) [20] within a certain range:

$$R_{\mathrm{LPPP}} = \frac{E_{\mathrm{LPP}}}{E_n} < \varepsilon, \tag{16}$$

where E_{LPP} and E_n are the loss of produced power and the total dispatching demand, respectively; and ε is the maximum reference loss of power supply probability of the unit.

(3) Wind-PV Complementary Constraint. The overall output power can be kept stable, and the number of charge-discharge as well as the discharge depth of the battery devices can be reduced by applying wind-PV complementation.

Consider

$$D_{\mathrm{wp}} = \frac{1}{P_{\mathrm{ref}}} \sqrt{\frac{1}{T}\sum_{t=1}^{T}\left(P_{\mathrm{wd\_PV}}(t) - P_{\mathrm{ref}}\right)^2} < \lambda, \tag{17}$$

where D_{wp} is the wind-PV output power/expected dispatching output power, $P_{\mathrm{wd\_PV}}$ is the wind-PV output power at t, and λ is the maximum reference fluctuation ratio of wind-PV complementation.

4. The Hybrid Iteration/Adaptive Genetic Algorithm

4.1. Basic Idea of the Algorithm. The optimal capacity allocation of large-scale wind-PV-battery unit was solved through iteration/adaptive hybrid genetic algorithm. This algorithm is divided into 2 stages as follows.

Stage 1. On the basis of the specification parameters of equipment, meteorological conditions, and expected dispatching output power and taking formulas (1)–(11) as the constraints of the equipment and formulas (15)–(17) as the constraints of the global performance, the iteration method was adopted to calculate the feasible solutions and feasible solution set PSS satisfying the system performance indexes.

Stage 2. On the basis of the elements and economic parameters in PSS and taking formulas (13)-(14) as objective function, adaptive genetic algorithm was utilized to solve the optimal capacity allocation result from PSS.

4.2. Improved Adaptive Genetic Algorithm. Genetic algorithm was firstly proposed by Professor Holland in University of Michigan in 1975 [21]. This algorithm searches for an optimal solution by simulating the natural evolutionary process which can offset nondifferentiation and discontinuity of functions. In consideration of abundant variables, a discontinuous variable domain of definition, multiple constraints, and other characteristics of the optimal capacity allocation model of wind-PV-battery unit, genetic algorithm owns obvious advantage to solve its optimal capacity allocation issue. However, a lot of studies and practices have demonstrated that the traditional genetic algorithm has poor local search capacity, premature convergence, and other defects. To solve the above problems, Srinivas and Patnaik proposed adaptive genetic algorithm which could dynamically adjust crossover probability p_C and mutation probability p_M according to the changes of fitness [22]. This paper adopted hybrid iterative/genetic algorithm from Khatib et al. [15] and Neungmatcha et al. fuzzy logic control method to dynamically adjust p_C and p_M and improve from group initialization, selection, crossover, mutation, and other aspects [23]. In this way, the convergence rate can be speeded up, the search efficiency can be optimized, and further the locally optimal solution can be avoided.

(1) Individual Coding. Binary coding was used to express three optimization variables, the numbers of wind generators, PV modules, and batteries. The lengths of these three optimization variables can be determined according to the constraints, which will be connected together to form an integral L_{wpb} long binary coding, shown as in Figure 4.

(2) Generation of Initial Group. Guaranteeing the variety of initial group contributes to the search of the whole solution space of the algorithm and avoids the premature convergence. This paper adopted the absolute Hamming distance $H(x_i, x_j)$ between different individuals as the measurement of group in the individual distribution and the Hamming distance between all the individuals in the group was required $H(x_i, x_j)$ $(i, j = 1, 2, \ldots, L_{\mathrm{wpb}}, i \neq j) \geq D$. At this time, the group size N_{Group} with individual length of L_{wpb} was noted as $2L_{\mathrm{wpb}} - D + 1$. Distance D was determined by the complexity of the issue and generally it fell approximately between 30 and 200.

(3) Selection Strategy. Selection, crossover, mutation, and other random operations may destroy the optimal individual in the current group which may have adverse effects on the operating efficiency and convergence. This paper utilized the elitist retention mechanism to keep the individuals with stronger fitness to the next group. At the same time,

there was common competition between the parent group and offspring group and they were ordered from stronger fitness to poor ones. The high-quality individuals in the former proportion of P_{CH} can be directly copied to the next generation.

(4) Adaptive Crossover and Variation Operator. The traditional genetic algorithm sets the constant values of crossover and mutation probability. Thus, the values of crossover and mutation probabilities usually greatly affect the search efficiency of the algorithm. Thus, this paper adopted Neungmatcha fuzzy logic control method to dynamically adjust the genetic operators to enable crossover probability p_C and mutation probability p_M to adjust with the changes of individual fitness relative to average group fitness. The adjustment method is as follows:

$$\begin{aligned}
\Delta \text{fit}_{\text{avg}}(t) &= \frac{1}{\text{popSize}} \sum_{k=1}^{\text{popSize}} \text{fit}_k(t) - \frac{1}{\text{offSize}} \sum_{k=1}^{\text{offSize}} \text{fit}_k(t), \\
\Delta c(t) &= \alpha \times Z(i,j), \qquad \Delta m(t) = \beta \times Z(i,j), \\
p_C(t) &= \Delta c(t) + p_C(t-1), \\
p_M(t) &= \Delta m(t) + p_M(t-1),
\end{aligned} \tag{18}$$

where $\Delta \text{fit}_{\text{avg}}(t)$ is the average fitness of t-generation group; Δc and Δm are offset of crossover and variation; popSize and offSize are parent group size and offspring group size; k is the particle ID; α and β are the maximum offset range of each crossover and variation; and $Z(i, j)$ is the fuzzy control rule, which is determined by $\Delta \text{fit}_{\text{avg}}(t)$ and $\Delta \text{fit}_{\text{avg}}(t-1)$.

4.3. Steps of the Algorithm

Stage 1

Step 1. Obtain meteorological data, specifications of equipment, and system expected output power data. Set the value range of optimization variables to reduce the cycle times of iterative algorithm. Among them, the lower limit of wind unit and PV unit is set as 1 while their upper limit is constrained by the planned site and $P_{\text{wd}}N_{\text{wd}} + P_{\text{PV}}N_{\text{PV}} > P_{\text{ref}}$. The lower limit of the number of batteries is set as 1 and its upper limit is set as $P_{\text{ref}}/P_{\text{bat}}$.

Step 2. Preset ε, λ and calculate each capacity combination to obtain the feasible solutions satisfying the constraints. Also, the system performance indexes of each group are gathered, for example, service hours of wind generator, gross generation, charge-discharge times of battery, and loss of power supply probability.

Stage 2

Step 1. Obtain feasible solution set, corresponding system performance indexes, and economic parameters. Code each set of feasible solutions according to Figure 4 and set the minimum group Hamming distance as D. Obtain the initial values of the group size (N_{Group}), the number of iterations (Iter), proportion of high-quality individuals (P_{CH}), crossover probability (p_C), and mutation probability (p_M). The initial group (G) is gained.

Step 2. According to formulas (13)-(14), calculate the economic efficiency of individual capacity allocation plan. In consideration of the energy waste and wind-PV complementation, the individual fitness is calculated according to formula (19).

One has

$$\text{Fit}(x) = \frac{1}{C_{\text{NPC}}(x) + \lambda_1 R_{\text{LPSP}} + \lambda_2 D_{\text{wp}} + 1}, \tag{19}$$

where λ_1 and λ_2 are loss of produced power probability and penalty coefficient of wind-PV complementation.

According to the selection strategy and crossover and mutation strategy in Section 4.2, the group is updated and G_i is got.

Step 3. Judge whether the terminal condition of the algorithm is satisfied. If not, turn to Step 2. If so, select the individual G_{Iter} with the strongest fitness and output capacity allocation plan $X' = [N'_{\text{wd}} \quad N'_{\text{PV}} \quad N'_{\text{bat}}]^T$ and costs of each unit as well as the overall performance index of the system. The procedure of the algorithm was shown in Figure 5.

5. Case Study

5.1. Basic Data. A simulation calculation was conducted in Zhangbei county, Zhangjiakou city, Hebei province. Zhangbei is located in 114°21′E to 114°27′E, 40°59′N to 41°07′N, and meteorological condition data in 2003 were used. The expected constant dispatching output power was set as P_{ref} = 100 MW and the specification parameters of equipment, economic parameters, and algorithm parameters were shown as in Tables 1, 2, and 3. PV panels of the same type are connected to the independent inverter chamber to form PV unit. Battery energy storage unit is formed by connecting several battery cabinets into a battery pack series and then connecting other battery pack series in parallel. The division of PV unit and energy storage unit is good for the operators' control of the large-scale power generation unit.

5.2. Optimization Results and Analysis

(1) The Optimization Results Analysis. A simulation was conducted based on the proposed optimal capacity allocation. The final optimization results are shown in Figures 6 to 8.

Figure 6 presents the wind-PV output power curve and the overall output power curve of the wind-PV-battery unit in a year. Under a fixed coordinated operation and control strategy, the wind-PV-battery unit can output constant power at any time, thus ensuring stable grid-connected operation of renewable energy sources. Table 4 lists the optimal capacity allocation: 242 MW for the wind generator, 81 MW for the PV module, and 72 MW for the battery, thus showing

Table 1: Specification parameters of equipment.

Wind generator		PV module		Battery	
Parameter	Value	Parameter	Value	Parameter	Value
Serial no.	GW2000A	Serial no.	STP300	Model no.	KYN61
Rated power (MW)	2.0	Peak power (MWp)	0.5	Rated capacity (MW·h)	1
Cut-in wind speed (m/s)	4.3	Open-circuit voltage (V)	44.6	Maximum charge depth (%)	70
Rated wind speed (m/s)	10.8	Short-circuit current (A)	8.33	Charge efficiency (%)	90
Cut-out wind speed (m/s)	25.6	Size (mm)	1966 × 982 × 50	Nominal voltage (KV)	40.5
Hub height (m)	80	Peak temperature coefficient (°C)	−0.47%	Maximum power (MW)	1

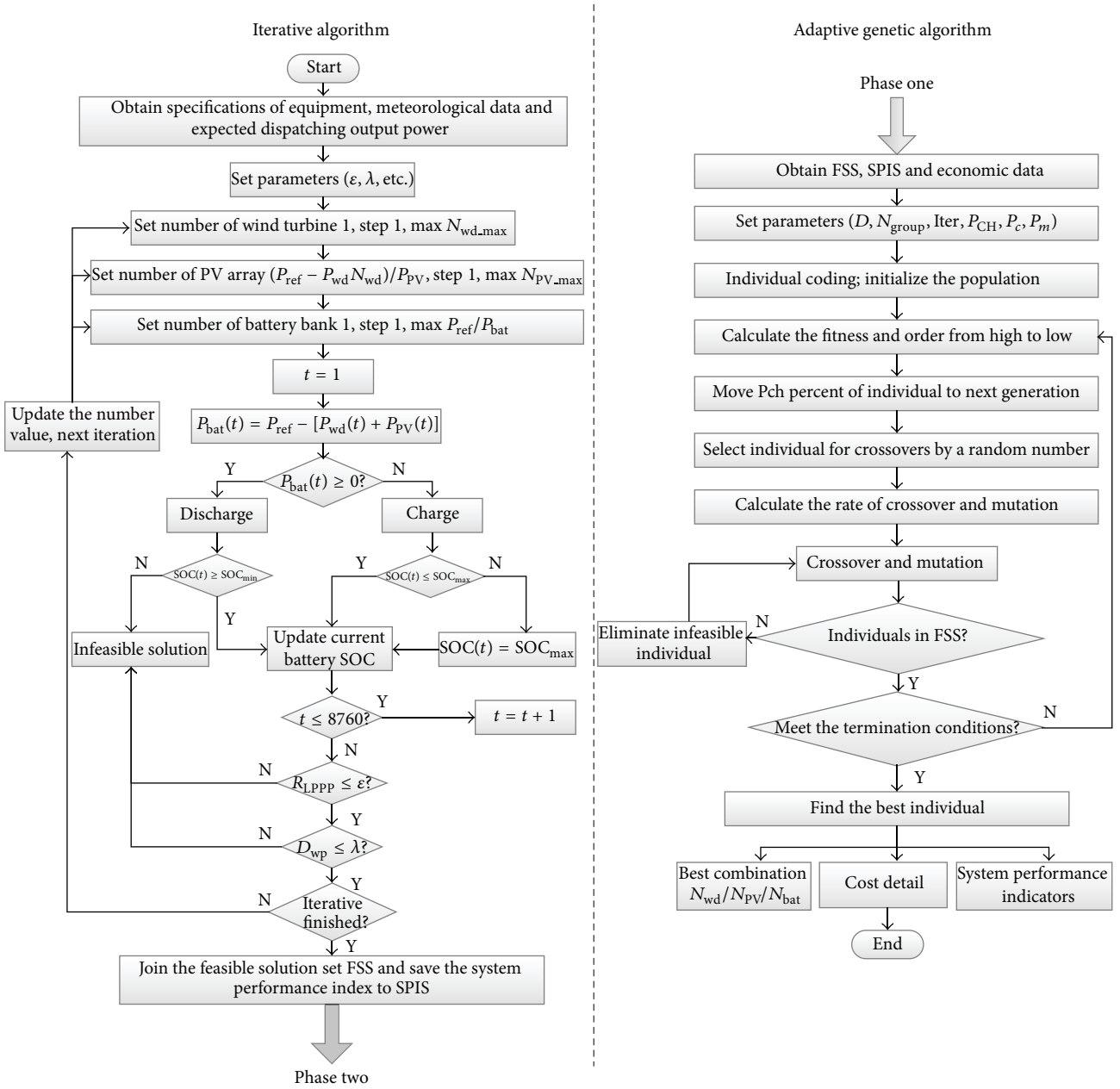

Figure 5: The HIAGA procedure.

Table 2: Economic parameters.

Equipment no.	Price (US$)	Operating maintenance cost (US$/Y)	Downtime maintenance cost (US$/Y)	Feed-in tariff (US$/KW·h)
GW2000A	1,370,000	6,000	4,000	0.14
STP300	750,000	3.7	1.2	0.19
KYN61	950,000	8,000	1,600	0.11

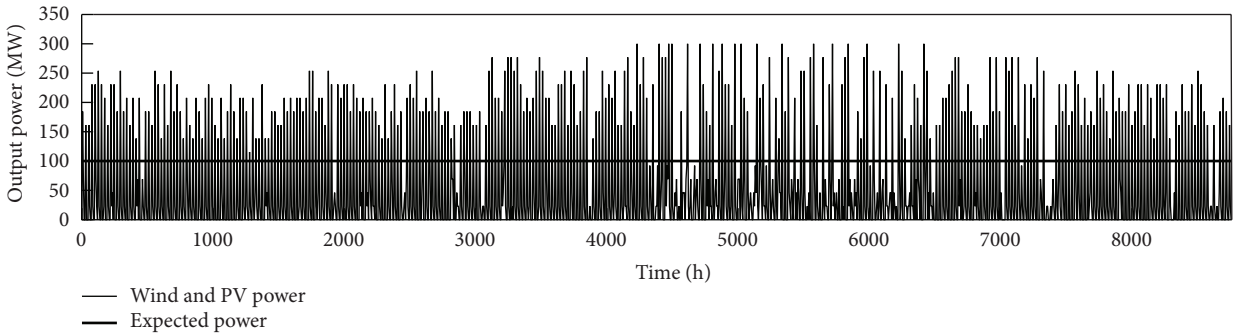

Figure 6: Annual output power curve of the wind-PV-battery unit.

Table 3: HIAGA parameters.

Index	Parameter value
Iter	60
N_{Group} (L_{wpb})	30~200
P_{CH} (%)	5
λ	1.5
ε (%)	10
λ_1	5×10^8
λ_2	2×10^8

a ratio of 0.61 : 0.21 : 0.18. Based on these values, the wind generator has a relatively higher installed capacity compared with the PV module and the battery. The local output power curve of the wind-PV-battery unit (Figure 7) explores the reason for the higher installed capacity of the wind generator in Zhangbei county. Zhangbei county has rich and even wind resources throughout the year, thus resulting in strong matching between the output power of the wind generator and the expected dispatching demand. Solar resources have less dispatching demand because they are only available during daytime. In particular, during the summer rainy season sunlight time shortens but temperature increases, thus significantly decreasing the energy conversion efficiency of PV modules and decreasing PV output.

According to the comparison of electricity generation (Figure 8), wind is the major source of electricity generation and PV is used nearly equally throughout the year, whereas battery is mainly used during summer. Further analysis (Figures 9-10) demonstrates frequent battery charge-discharge from June to August because weather changes often during the rainy season. Consequently, the wind-PV output fluctuates violently, thus requiring the battery to charge and discharge frequently to smooth power fluctuation and to ensure the constant output of the wind-PV-battery unit.

(2) Contrastive Analysis with Hocaoglu Optimization Algorithm [24]. The capacity allocation results under the condition of 100 MW expected output power of the optimization algorithm proposed in this paper and Hocaoglu optimization algorithm are shown as Table 4. It can be seen from the comparative results that the installed capacity of wind unit allocated by Hocaoglu optimization algorithm was higher than those of PV and battery units. The reason is that, in Hocaoglu optimization computation process, the model of battery life cycle was not established. Instead, it was simplified into a replacement every 5 years. Furthermore, this method did not consider the influence of wind-PV power output fluctuation range on the life cycle of battery. This kind of allocation had a lower initial investment cost while the accuracy degree of the model was poorer. As seen from the total investment cost in Table 4, compared with the optimization algorithm proposed in this paper, Hocaoglu optimization algorithm decreased 1.2% but its total investment cost of the entire project term may not be optimal. Table 5 provides the costs of each unit through simulation calculation on the basis of 2003–2013 meteorological data. It can be seen from the cost details in Table 5 that the initial investment and construction year was 2003. Thus, the costs of both algorithms in 2003 were high and the costs left years were constituted of operation costs and replacement costs. Every 5 years, there was one peak in cost for Hocaoglu optimization algorithm which was related to the 5-year life cycle of battery. The annual expense of the optimization algorithm proposed in this paper was average and there was no large-scale battery replacement. During the allocation process, this method fully considered wind-PV complementation, which contributed to decreasing the wind-PV output fluctuation range and

Table 4: The contrast of optimal configuration result.

Optimizer	Wind turbine		PV unit		Battery unit		Total	
	Number	Capacity (MW)	Number	Capacity (MW)	Number	Capacity (MW)	Ratio	Cost (US$)
Hocaoglu	129	258	144	72	70	70	0.65 : 0.18 : 0.17	351,230,000
Proposed	121	242	162	81	72	72	0.61 : 0.21 : 0.18	355,670,000

Table 5: The comparison of cost detail.

Year	Hocaoglu			Proposed		
	Expense (US$)	Income (US$)	NPC (US$)	Expense (US$)	Income (US$)	NPC (US$)
2003	360,369,200	12,210,800	331,579,400	364,809,200	12,755,100	335,289,600
2004	3,846,600	11,780,100	−7,195,900	3,380,800	13,483,300	−9,163,265
2005	2,532,500	13,283,900	−9,287,400	2,979,000	12,869,600	−8,543,800
2006	2,332,600	13,344,700	−9,059,600	4,021,500	12,719,300	−7,155,700
2007	9,687,600	12,424,100	−2,144,100	3,994,000	11,925,700	−6,214,600
2008	2,019,500	11,699,800	−7,223,500	2,461,800	12,691,600	−7,633,600
2009	3,464,900	12,710,000	−6,570,300	3,459,100	13,150,900	−6,887,700
2010	3,450,700	13,256,800	−6,637,100	4,017,300	13,090,200	−6,140,800
2011	2,702,300	11,858,600	−5,902,200	2,511,100	13,370,200	−6,999,800
2012	9,457,500	11,795,300	−1,435,200	2,998,500	11,809,400	−5,409,100
2013	2,031,000	11,920,000	−5,781,800	2,553,500	13,101,200	−6,167,000
Total	401,894,400	136,284,100	270,341,800	397,185,800	140,966,500	264,973,700

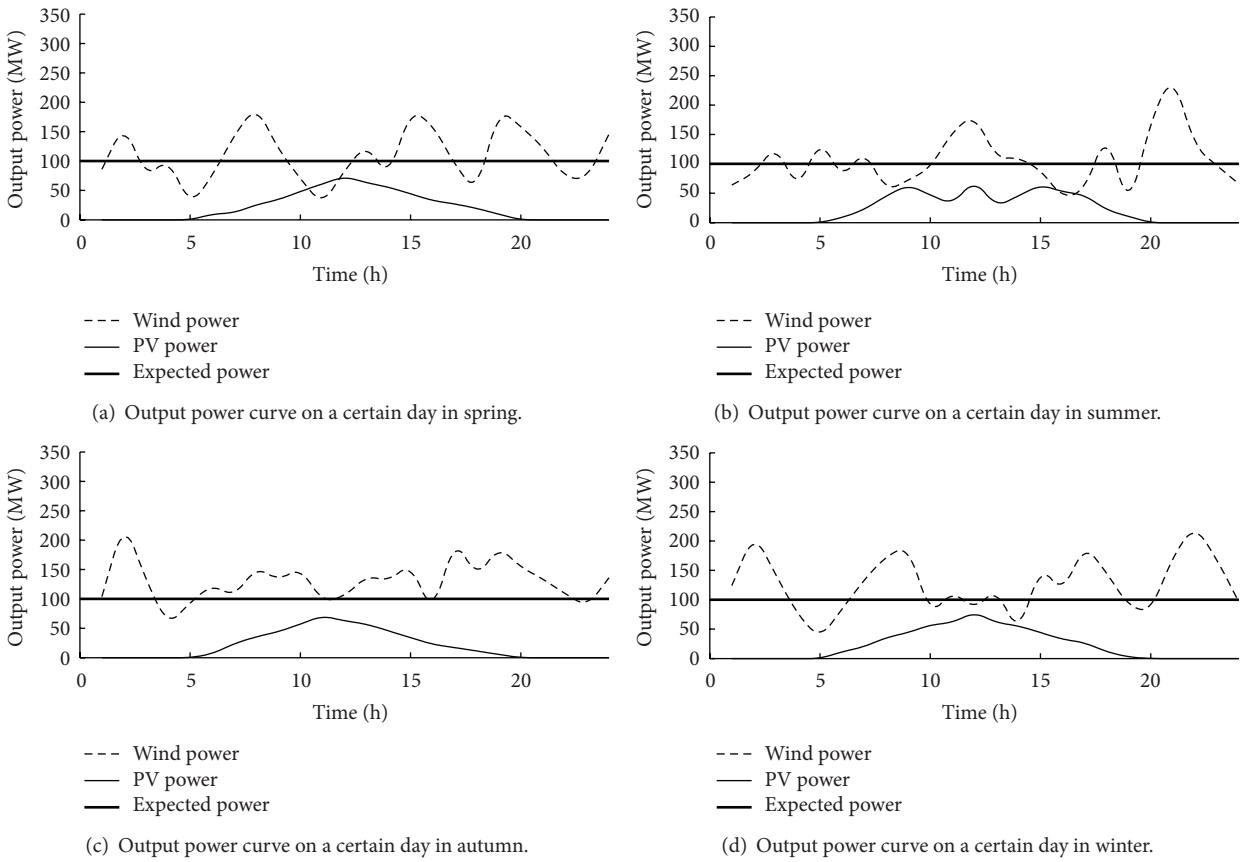

(a) Output power curve on a certain day in spring.

(b) Output power curve on a certain day in summer.

(c) Output power curve on a certain day in autumn.

(d) Output power curve on a certain day in winter.

Figure 7: Output power curve on a certain day in different season.

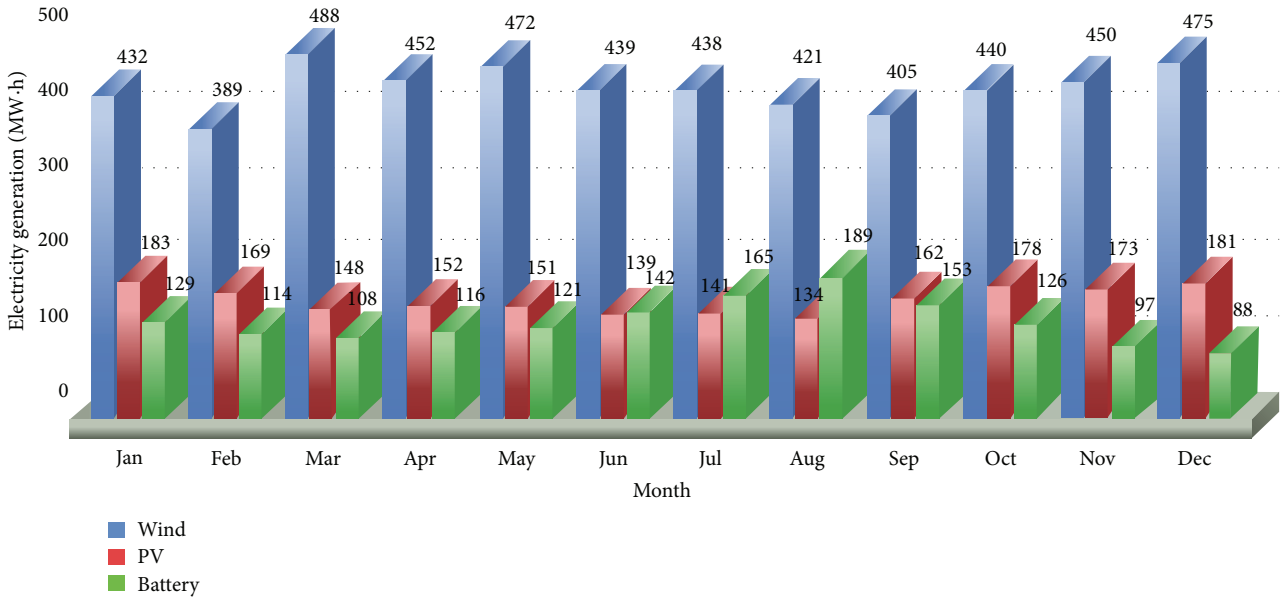

Figure 8: Comparison of the monthly electricity generation of wind, PV, and battery.

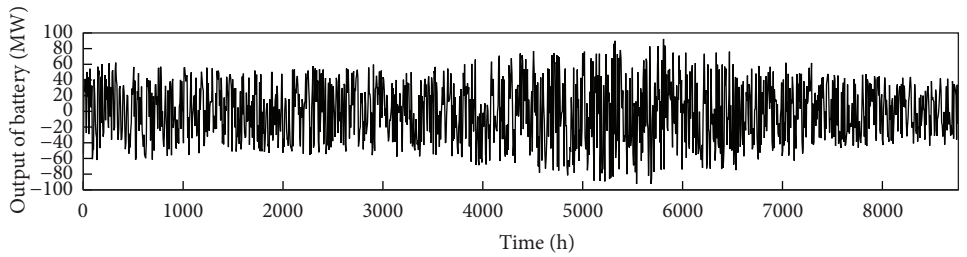

Figure 9: Output power curve of the battery.

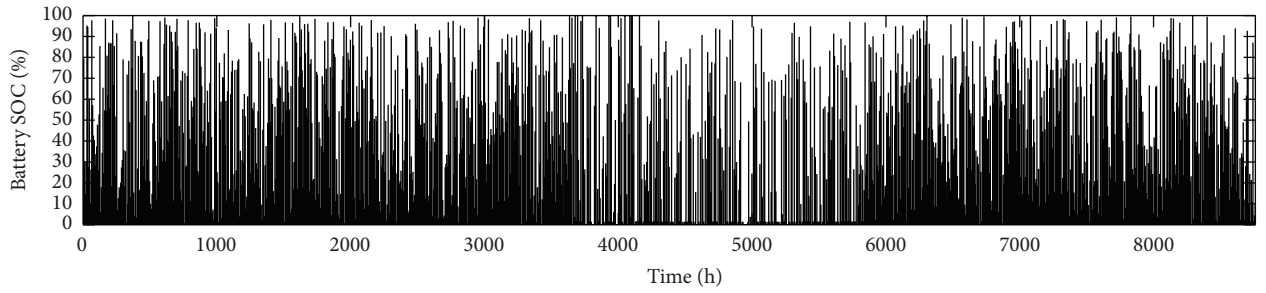

Figure 10: Battery SOC.

frequency, the charge-discharge times, and discharge depth of battery, which could extend the life cycle of battery and minimize the total cost in the whole life cycle. From the aggregated data in the last line of Table 5, it can be seen that the total costs of the optimization algorithm proposed in this paper were 397,185,800 (US.$), 1.2%, lower than that of Hocaoglu optimization algorithm. Its NPC was 264,973,700 (US.$), decreasing by 2%.

Table 6 shows the system performance indexes through simulation calculation on the basis of 2003–2013 meteorological data. It is found that each index of the optimization algorithm proposed in this paper was superior to that of Hocaoglu optimization algorithm. Among them, loss of power supply probability was 6.57%, decreasing by 21.4%; wind-PV complementation was 1.22, increasing by 11.6%; charge-discharge times of battery were 676,548, decreasing by 7.5%; levelized cost of energy was 0.215 (US$/KW·h), decreasing by 3.6%.

(3) Convergence Analysis of the Algorithm. To make an objective and overall evaluation of the optimization algorithm proposed in this paper, Hocaoglu optimization algorithm,

Table 6: Performance indicators.

Indicator	Hocaoglu	Proposed
Loss of produced power probability (%)	8.36	6.57
Wind-PV complementation characteristics	1.38	1.22
Number of battery charge-discharge	730,997	676,548
LCE (US$/KW·h)	0.223	0.215

Khatib optimization algorithm [15], and the optimization algorithm proposed in this paper, respectively, carried out 30 simulations. Through the changes of the parameters of the algorithm, the group number and CPU computation time at the beginning of convergence were observed and gathered (shown as in Table 7). It can be seen that HIAGA optimization algorithm was the fastest and started convergence at 22nd-generation group and its average convergence algebra was 27.6, respectively, 30.5% and 20% higher than Hocaoglu optimization algorithm and Khatib optimization algorithm. In terms of CPU computation time, the average convergence time of HIAGA optimization algorithm was 85.8 s, respectively, 10.6% and 6.4% higher than Hocaoglu optimization algorithm and Khatib optimization algorithm. These indicated that the convergence rate of HIAGA optimization algorithm was faster and it owned certain advantages compared with the previous research results.

5.3. Sensitivity Analysis

(1) Potential Wind-PV Resources. Through simulations in several regions in China, the optimal capacity allocation and costs of each component of the wind-PV-battery unit, when $P_{ref} = 100$ MW were calculated as shown in Table 8, and large-scale wind-PV-battery units in regions with rich wind resources have high economic efficiency because wind-dominated units require less capacity for cost-ineffective battery (high cost but short life cycle) compared with PV-dominated units. Furthermore, the even distribution of wind power and appropriate PV output complementation enable the entire wind-PV-battery unit to maintain a constant output with only a small battery capacity.

(2) Government Support. China is experiencing an increasing number of hazy days because of the continuously worsening environment. Consequently, the country is paying significant attention to the development of green energies. However, wind-PV-battery power generation is inferior to thermal power generation because of its lower economic efficiency. As such, the government should formulate reasonable energy policies to support the development of new energy-based power enterprises. At present, numerous countries worldwide support wind power and PV power generation. China also adopted a fixed electricity price and increased subsidies to PV power generation in 2008. However, no policy about the feed-in tariff of battery power has yet been released. The relationship curve between the feed-in tariff of battery power and the NPC of the wind-PV-battery unit is presented in Figure 11.

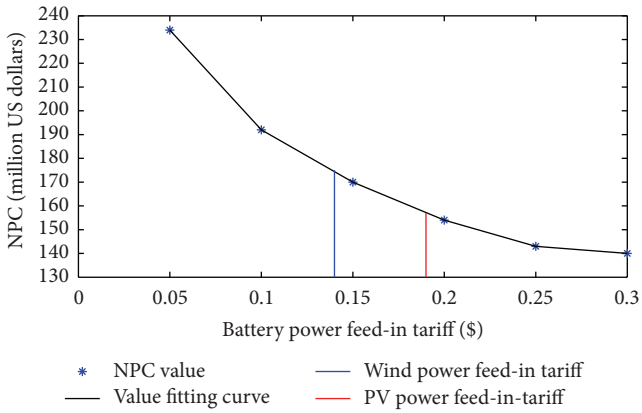

Figure 11: Impact of the feed-in tariff of battery power.

According to Figure 11, the NPC of the wind-PV-battery unit is more sensitive to the feed-in tariff of battery power when the latter is smaller than the feed-in tariffs of wind power and PV power. This finding is attributed to the low economic efficiency of battery power. Moreover, each charge-discharge requires high investment costs, thus significantly affecting the NPC. When the feed-in tariff of battery power exceeds those of wind power and PV power, the optimal capacity allocation will involve an extremely large proportion of battery energy to absorb all wind-PV electricity, thus influencing the NPC slightly. However, this process violates the practical significance of the wind-PV-battery unit.

6. Conclusion

This study proposes an optimal capacity allocation of a large-scale wind-PV-battery unit, in which the wind-PV-battery power-generation system is connected to the power grid as a power-generating unit with a fixed rated capacity. This feature does not only ensure the stable output of the wind-PV-battery unit, but is also convenient to the power grid for evaluating the power-generation capacity of the wind-PV-battery unit, thus formulating a corresponding dispatching plan and increasing acceptance of renewable energy sources. Aiming at minimum NPC and considering power distribution reliability, energy utilization rate, and other indexes, the iteration/adaptive hybrid genetic algorithm was used to solve the optimal capacity ratio of each component in the wind-PV-battery unit and a simulation analysis on the wind-PV-battery unit with a construction rated capacity of 100 MW in Zhangbei county (China) was carried out. Then the comparative results between Hocaoglu optimization algorithm and HIAGA optimization algorithm indicated that HIAGA optimization algorithm could minimize the investment cost of the entire life cycle of the power-generation unit project and the accuracy and validity of the model and algorithm were also verified. Through the multiple simulation calculations, the optimization algorithm proposed in this paper owned faster convergence rate and search efficiency than Hocaoglu and Khatib optimization algorithm. Finally, the sensitivity analysis of the large-scale wind-PV-battery unit determines

Table 7: The algorithm convergence analysis.

Optimizer	Convergence at generation k			CPU times of convergence(s)		
	Minimum	Maximum	Average	Minimum	Maximum	Average
Hocaoglu	28	54	39.7	92.3	116.1	96.0
Khatib	29	39	34.5	86.9	114.6	91.7
Proposed	22	31	27.6	82.1	94.3	85.8

Table 8: Comparative analysis of allocations in different regions.

Region	Annual average wind speed (m/s)	Annual average illumination intensity (W/m^2)	Annual average temperature (°C)	Capacity allocation ($N_{wd}/N_{PV}/N_{bat}$)	NPC (US$)
Zhangbei	6.6	1040	2.6	$121/2.7 \times 10^5/72$	188,274,000
Chifeng	6.1	980	1.9	$126/2.95 \times 10^5/82$	197,463,000
Tangshan	3.6	1270	5.8	$82/5.94 \times 10^5/172$	422,198,000
Datong	4.1	1210	2.9	$95/5.31 \times 10^5/156$	387,579,000
Baotou	6.4	1025	2.2	$82/2.95 \times 10^5/82$	195,387,000

that wind-solar resources and government energy policies have a significant effect on the economic efficiency of the unit. The wind-PV-battery unit in regions with rich wind resources requires less battery capacity compared with that in regions with rich solar resources, thus exhibiting higher economic efficiency. A reasonable feed-in tariff for battery power imposed by the government can improve the economic benefits of new energy-based power enterprises. The results of the sensitivity analysis also confirm the accuracy of the proposed model and algorithm.

Conflict of Interests

The authors declare that there is no conflict of interests regarding the publication of this paper.

Acknowledgment

The authors would like to acknowledge the support from the State Key Laboratory of Alternate Electrical Power System with Renewable Energy Sources (North China Electric Power University).

References

[1] S. Rehman, M. Mahbub Alam, J. P. Meyer, and L. M. Al-Hadhrami, "Feasibility study of a wind-pv-diesel hybrid power system for a village," *Renewable Energy*, vol. 38, no. 1, pp. 258–268, 2012.

[2] J. S. Silva, A. R. Cardoso, and A. Beluco, "Consequences of reducing the cost of PV modules on a PV wind diesel hybrid system with limited sizing components," *International Journal of Photoenergy*, vol. 2012, Article ID 384153, 7 pages, 2012.

[3] D. Amorndechaphon, S. Premrudeepreechacharn, K. Higuchi et al., "Modified grid-connected CSI for hybrid PV/wind power generation system," *International Journal of Photoenergy*, vol. 2012, Article ID 381016, 12 pages, 2012.

[4] M. Engin, "Sizing and simulation of PV-wind hybrid power system," *International Journal of Photoenergy*, vol. 2013, Article ID 217526, 10 pages, 2013.

[5] G. Mingjie, H. Dong, G. Zonghe et al., "Presentation of national wind/photovaltaic/energy storage and transmission demonstration project and analysis of typical operation modes," *Automation of Electric Power Systems*, vol. 37, no. 1, pp. 59–64, 2013.

[6] M. Mohammadi, S. H. Hosseinian, and G. B. Gharehpetian, "Optimization of hybrid solar energy sources/wind turbine systems integrated to utility grids as microgrid (MG) under pool/bilateral/hybrid electricity market using PSO," *Solar Energy*, vol. 86, no. 1, pp. 112–125, 2012.

[7] H. Yang, Z. Wei, and L. Chengzhi, "Optimal design and techno-economic analysis of a hybrid solar-wind power generation system," *Applied Energy*, vol. 86, no. 2, pp. 163–169, 2009.

[8] H. Yang, W. Zhou, L. Lu, and Z. Fang, "Optimal sizing method for stand-alone hybrid solar-wind system with LPSP technology by using genetic algorithm," *Solar Energy*, vol. 82, no. 4, pp. 354–367, 2008.

[9] H. Yang, L. Lu, and W. Zhou, "A novel optimization sizing model for hybrid solar-wind power generation system," *Solar Energy*, vol. 81, no. 1, pp. 76–84, 2007.

[10] S. Diaf, G. Notton, M. Belhamel, M. Haddadi, and A. Louche, "Design and techno-economical optimization for hybrid PV/wind system under various meteorological conditions," *Applied Energy*, vol. 85, no. 10, pp. 968–987, 2008.

[11] H. A. Kazem and T. Khatib, "A novel numerical algorithm for optimal sizing of a photovoltaic/wind/diesel generator/battery microgrid using loss of load probability index," *International Journal of Photoenergy*, vol. 2013, Article ID 718596, 8 pages, 2013.

[12] J. Li, W. Wei, and J. Xiang, "A simple sizing algorithm for stand-alone PV/wind/battery hybrid microgrids," *Energies*, vol. 5, no. 12, pp. 5307–5323, 2012.

[13] R. Dufo-López, J. L. Bernal-Agustín, J. M. Yusta-Loyo et al., "Multi-objective optimization minimizing cost and life cycle emissions of stand-alone PV-wind-diesel systems with batteries storage," *Applied Energy*, vol. 88, no. 11, pp. 4033–4041, 2011.

[14] R. Dufo-López and J. L. Bernal-Agustín, "Multi-objective design of PV-wind-diesel-hydrogen-battery systems," *Renewable Energy*, vol. 33, no. 12, pp. 2559–2572, 2008.

[15] T. Khatib, A. Mohamed, and K. Sopian, "Optimization of a PV/wind micro-grid for rural housing electrification using a

hybrid iterative/genetic algorithm: case study of Kuala Terengganu, Malaysia," *Energy and Buildings*, vol. 47, pp. 321–331, 2012.

[16] F. O. Hocaoglu, O. N. Gerek, and M. Kurban, "The effect of model generated solar radiation data usage in hybrid (wind-PV) sizing studies," *Energy Conversion and Management*, vol. 50, no. 12, pp. 2956–2963, 2009.

[17] B. Li, H. Shen, Y. Tang, and H. Wang, "Impacts of energy storage capacity configuration of HPWS to active power characteristics and its relevant indices," *Power System Technology*, vol. 35, no. 4, pp. 123–128, 2011.

[18] H. Wenzl, I. Baring-Gould, R. Kaiser et al., "Life prediction of batteries for selecting the technically most suitable and cost effective battery," *Journal of Power Sources*, vol. 144, no. 2, pp. 373–384, 2005.

[19] L. Mengxuan, W. Chengshan, G. Li et al., "An optimal design method of multi-objective based island microgrid," *Automation of Electric Power Systems*, vol. 36, no. 17, pp. 34–39, 2012.

[20] G. Xydis, "On the exergetic capacity factor of a wind-solar power generation system," *Journal of Cleaner Production*, vol. 47, pp. 437–445, 2012.

[21] J. H. Holland, *Adaptation in Natural and Artificial Systems: An Introductory Analysis with Applications to Biology, Control, and Artificial Intelligence*, The University of Michigan Press, 1975.

[22] M. Srinivas and L. M. Patnaik, "Adaptive probabilities of crossover and mutation in genetic algorithms," *IEEE Transactions on Systems, Man and Cybernetics*, vol. 24, no. 4, pp. 656–667, 1994.

[23] W. Neungmatcha, K. Sethanan, M. Gen et al., "Adaptive genetic algorithm for solving sugarcane loading stations with multi-facility services problem," *Computers and Electronics in Agriculture*, vol. 98, pp. 85–99, 2013.

[24] F. O. Hocaoğlu, Ö. N. Gerek, and M. Kurban, "A novel hybrid (wind-photovoltaic) system sizing procedure," *Solar Energy*, vol. 83, no. 11, pp. 2019–2028, 2009.